



Formation of Multi-Walled Carbon Nanotubes by Catalytic Chemical Vapour Deposition Using Zeolite Encapsulated Nanocrystalline Cobalt Oxides

WEI ZHAO^{1*}, MI JAI LEE², HYUNG TAE KIM², YOO JIN KIM², JIANGHONG GONG³ and IK JIN KIM^{1*}

¹Institute for Processing and Application of Inorganic Materials, Department of Materials Science and Engineering, Hanseo University, 360 Daegok-ri, Haemi-myun, Seosan city 356-706, Chungnam, South Korea

²Engineering Ceramic Center, Korea Institute of Ceramic Engineering and Technology, Icheon 467-84, Kyoung-gi do, South Korea

³Department of Materials Science and Engineering, Tsinghua University, Beijing 100084, P.R. China

*Corresponding authors: Tel/Fax: +82 41 6601441; E-mail: zhao-w05@mails.tsinghua.edu.cn; ijkim@hanseo.ac.kr

(Received: 22 February 2011;

Accepted: 24 August 2011)

AJC-10305

High yield multiwalled carbon nanotubes (MWNTs) were synthesized on Co-supported faujasite-type zeolite (FAU) by catalytic chemical vapour deposition (CCVD) using acetylene as the carbon source. Well-shaped faujasite-type zeolite (FAU) octahedral crystals of a size of 15 μm were synthesized by the hydrothermal method in a mother solution which has a composition of 3.5 $\text{Na}_2\text{O} : \text{Al}_2\text{O}_3 : 2.1 \text{SiO}_2 : 1000 \text{H}_2\text{O}$. The effect of the Co content in the zeolite crystals on the synthesis of carbon nanotubes was investigated through high resolution transmission electron microscopy (HRTEM), field emission microscopy (FESEM), thermogravimetric analysis (TGA) and Raman spectroscopy. The inner and outer tube diameters of the synthesized multiwalled carbon nanotubes were in the range of 5.7-11.6 nm and 11.0-30.2 nm, respectively. With increasing Co content supported in the zeolite template, the carbon yield showed a monotonic increasing tendency, reaching 60.4 % when the Co content was up to 11.5 wt%.

Key Words: Multi-walled carbon nanotubes, Chemical vapour deposition, Zeolite, Ion-exchange, Catalyst.

INTRODUCTION

Carbon nanotubes (CNTs), whose walls are made up of a hexagonal lattice of carbon atoms analogous to the atomic planes of graphite, are seamless cylinder-shaped macromolecules with a radius as small as a few nanometers, with their ends capped - or not - by one half of a fullerene-like molecule¹. In general, CNTs of a category are composed of a concentric arrangement of many cylinders, called multi-walled CNTs (MWNTs), of which a special case is the double-walled CNTs (DWNTs) composed of just two concentric cylindrical sheets. Another category involves single-walled CNTs (SWNTs), composed of a single layer of rolled-up graphene sheet².

Owing to their unique physical and chemical properties, CNTs are one of the exclusively studied 1D nanoscale materials that have attracted many interests in recent years and can be applied in many potential fields, such as chemical sensors and filters³, nanoelectronic devices⁴, composite materials⁵, hydrogen storage media⁶ and field emission devices⁷, etc.

However, if the price of CNTs still remains as high as today (e.g., US\$ 200/g for MWNTs to nearly 10 times this value for purified SWNTs)⁸, any large-scale application of CNTs will be unrealistic. Consequently, a simple and hence

low-cost synthesis of them with a controllable structure and high purity has become absolutely crucial to the development of the carbon nanoscience and nanotechnology.

Historically, chemical vapour deposition (CVD), especially catalytic chemical vapour deposition (CCVD) has proven to be much more effective and promising for CNTs synthesis because of its relatively low cost, simple operating conditions and potential high-yield production⁹, even though a complete understanding of the growth mechanism is still lacking at this time. In this method, CNTs are synthesized by the decomposition of a carbon feedstock (CH_4 , CO , C_2H_4 , etc.) over catalysts containing particles of transition metal (e.g., Fe, Co, Ni or their binary mixtures) or the related oxides, embedded in solid matrices or supported on the surfaces of porous materials. Nowadays, the employed catalytic supports or matrices comprise zeolites¹⁰, mesoporous silica¹¹, silica¹², alumina¹³ and so on. Among them, zeolites, with well-defined pore structures and high surface areas¹⁴, can act as hosts to support or encapsulate the catalytic transition metal, nanoparticles contributing significantly to their particle stabilization by preventing sintering, producing a fine dispersion of catalyst particles and increasing nucleation sites which is advantageous to high yield synthesis of CNTs¹⁵. Therefore, zeolite is a kind of catalyst support, which can contribute greatly to CNTs synthesis.

In this work, the faujasite-type zeolite NaX (FAU) is used as the template to support Co-containing particles with the ion-exchange method in aqueous solution in order to produce the catalyst for CNTs synthesis by CCVD. With the characterization by some methods, the dependence of the CNTs synthesis on cobalt contents which were supported in the same amount of zeolite is investigated.

EXPERIMENTAL

Preparation of the metal-supported zeolite catalyst:

First, the faujasite-type zeolite (FAU) crystals of 15 μm were synthesized by the hydrothermal method in a mother solution with a composition of 3.5 $\text{Na}_2\text{O} : \text{Al}_2\text{O}_3 : 2.1 \text{SiO}_2 : 1000 \text{H}_2\text{O}$. Second, the synthesized zeolite powder (1 g) was refluxed with aqueous solutions of cobalt(II)-chloride hexahydrate ($\text{CoCl}_2 \cdot 6\text{H}_2\text{O}$, analytical pure, $\geq 97.0\%$) by sufficient stirring for 24 h at approximately 30–40 $^\circ\text{C}$. The solutions were prepared by mixing $\text{CoCl}_2 \cdot 6\text{H}_2\text{O}$ powder of different masses (0.04, 0.08, 0.16 and 0.20 mol %) with deionized water of 250 mL. After stirring, the mixture was further centrifuged and washed thoroughly with pure ethanol ($\geq 99.9\%$). Co^{2+} cations were completely ion-exchanged as verified by SEM observation of the exchanged zeolite samples and by the colourless clear filtrate solution obtained after ion-exchanging. Ethanol was used instead of water to prevent the exchanged Co^{2+} cations from dissolving into the water again. The Co contents in the exchanged zeolite samples were approximately 2.35, 4.67, 9.25 and 11.5 wt%. Finally, the powder was dried at ambient temperature and calcined at 450 $^\circ\text{C}$ for 3 h in air prior to the catalytic decomposition of acetylene (C_2H_2). According to the cobalt content, four Co-supported zeolite samples were designated as CoNaX0, CoNaX1, CoNaX2 and CoNaX3.

Synthesis of CNTs: The CNTs were synthesized by catalytic decomposition of C_2H_2 on the calcined Co-supported zeolite in a fixed-bed flow reactor at atmospheric pressure. The reactor setup comprises a quartz boat containing the catalyst samples (approx 100 mg) which were placed in a horizontal electric tubular furnace. The catalysts were gradually heated from room temperature to 700 $^\circ\text{C}$ in a nitrogen (N_2) flow (500 sccm) and kept at this temperature for about 15 min. Then, a mixture of N_2 (200 sccm) and C_2H_2 (10 sccm) was subsequently fed into the reactor for 1 h, in order for the reaction to proceed. The furnace was then cooled to room temperature under N_2 flow (500 sccm) and produced CNTs were collected as a black powder from the quartz boat. All these CNT samples were denoted as CNT-CoNaX0, CNT-CoNaX1, CNT-CoNaX2 and CNT-CoNaX3.

Characterization: High resolution transmission electron microscopy (HRTEM) observations were carried out on a JEOL JEM-3011 at an accelerating voltage of 200 kV. Samples were prepared by evaporating drops of a zeolite-CNT-ethanol suspension after sonication onto a carbon-coated lacy film supported on a 3 mm diameter, 300 -mesh copper grid. Field emission scanning electron microscopy images were collected with a FESEM LEO 1530 VP microscope. Energy-dispersive X-ray analyses were acquired with this FESEM microscope equipped with an EDX detector. Thermogravimetric (TG) analysis was performed to measure the amount of carbon

deposited in the experiment and also to evaluate the percentage of other forms of carbon. It was conducted under air in a Seiko Extar 7300 (TG/DTA 7300) instrument, with samples of approximately 5 mg heated in air from 25 to 750 $^\circ\text{C}$, at a heating rate of 10 $^\circ\text{C}/\text{min}$. Raman spectroscopy measurements were performed with a Raman system FRA-106/S using a laser excitation line at 1064 nm (Nd-YAG) in the range of 50–2000 cm^{-1} .

RESULTS AND DISCUSSION

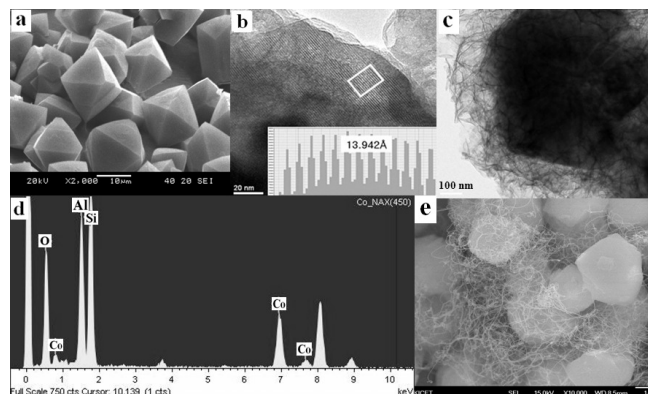


Fig. 1. (a) FESEM image of synthesized zeolite crystals, (b) HRTEM image of the zeolite crystal, (c) HRTEM image of catalyst sample CoNaX, (d) EDX data of the catalyst sample CoNaX and (e) FESEM image of CNTs synthesized from CoNaX

A previous study¹⁶ revealed that hydrothermally synthesized faujasite-type zeolite (FAU) crystals [Fig. 1(a)] have a high degree of structural order in the crystal surface formed inside the complementary pores between two distinct peaks, each centered at 13.942 \AA [Fig. 1(b)], corresponding to the inner diameter of the zeolite structure. They can be envisaged as a stack of layers of sodalite cages joined by double six rings (D6R) in a tetrahedral arrangement like the carbon atom in diamond, with a center of inversion at the center of the D6R. The β -cage is surrounded by an even larger cage, the supercage (cavity with a diameter of about 13 \AA), which forms a three-dimensional network with each cage connected tetrahedrally to four other supercages through the 12-membered ring opening with a crystallographic aperture of 7–8 \AA .

As shown in Fig. 1(c), after ion-exchanging, Co-containing catalyst nanoparticles suitably dispersed on the external surface of zeolite crystals. Moreover, there was no significant breakdown of the zeolitic structure after calcination and intense agglomeration of catalyst particles. Compared with synthesized zeolite crystals shown in Fig. 1(a), it can also be confirmed by EDX [Fig. 1(d)] test that the calcined Co-exchanged zeolite crystals showed no Na^+ ions at all, indicating that all the Na^+ ions have been completely exchanged with Co^{2+} ions during the ion-exchanging process. This result provides an obvious evidence of the function of zeolite as the excellent template for supporting catalyst particles, resulting in bundles of CNTs grown from Co-supported zeolite crystals, as shown by FESEM image in Fig. 1(e).

Fig. 2 shows HRTEM images of CNTs synthesized at 700 $^\circ\text{C}$ for 1 h from different Co contents supported zeolite. Clearly, the CNT products are typically MWNTs. Through the observation of the ensemble of synthesized CNTs, it is

easy to find that their inner diameters and outer diameters largely distribute in the range of 5.7-11.6 nm and 11.0-30.2 nm, respectively, with an interlayer distance of 0.34 ± 0.2 nm, indicating a similar interlayer spacing to that reported in the former study¹⁷. They could be formed at lower Co content as in catalyst sample CoNaX0 and exhibited a growth tendency in terms of their layer number of walls, length and yield with increasing Co content. This suggests that more catalyst particles found in the CNTs act as seeds for the CNT synthesis with increasing Co content, leading to the increasing CNT yield. Also because of the calcination, most Co was stabilized at the state of oxides, which to some extent destroys the zeolitic structure. Therefore, random dispersion of increasing catalyst nanoparticles leads to an intensive agglomeration, which results in increasing diameter and layer number of CNTs walls. This phenomenon is just in accordance with generally accepted theory that catalyst particle size determines the diameter of CNTs¹⁸.

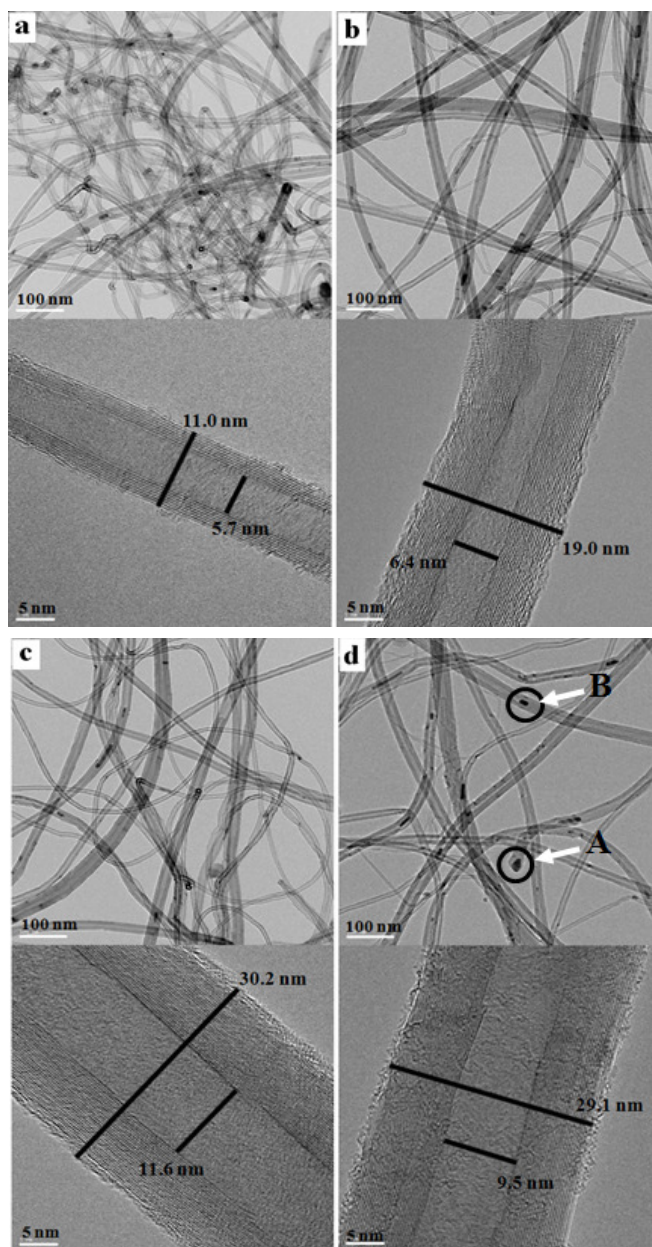


Fig. 2. HRTEM images of synthesized CNTs; (a) CNT-CoNaX0, (b) CNT-CoNaX1, (c) CNT-CoNaX2 and (d) CNT-CoNaX3

In addition, it is obvious that even after the synthesis of the CNTs, some of catalyst particles still remained in CNTs, which could be identified by the black spots inside CNTs circled and emphasized by arrows, as shown in typical HRTEM image Fig. 2(d), where A and B present catalyst particles at the tip and in the middle of CNTs, respectively. Similar to the previous study¹⁹, the result provides evidence that first, the diameters of CNTs are closely determined by the diameters of catalytic particles and second, TEM imaging of both ends of isolated CNTs points to the so-called tip-growth model of CNTs in CCVD process. That is, the carbon precipitation occurs at the bottom surface of the catalytic nanoparticles and the growing CNTs lift the particles as they grow. As can be seen, the top end of the CNT contains the catalyst particle [shown by A in Fig. 2(d)] and even the catalyst particle is not at the top end of the CNT, it locates in the middle of the CNT [shown by B in Fig. 2(d)] rather than adhere to the external surface of the catalyst.

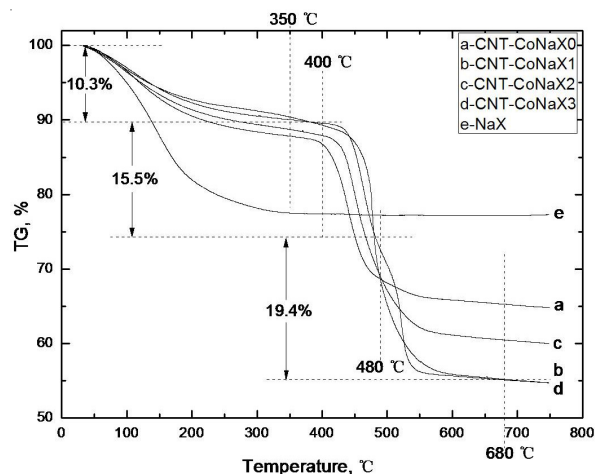


Fig. 3. TG curves of synthesized CNTs (a) CNT-CoNaX0, (b) CNT-CoNaX1, (c) CNT-CoNaX2, (d) CNT-CoNaX3 and (e) the synthesized zeolite (FAU)

Fig. 3 shows the TG curves of the hydrothermally synthesized zeolite (FAU) sample and synthesized CNTs, CNT-CoNaX0, CNT-CoNaX1, CNT-CoNaX2 and CNT-CoNaX3. It is obvious that the initial weight loss (up to 350 °C) for synthesized CNTs in this work is nearly half that for the zeolite, which is attributed to the loss of physically absorbed heavy water on the zeolite. This may be caused by the elimination of most of the water inside the catalyst during the CNTs synthesis. After this weight loss, all CNT samples undergo a single step weight loss (400-680 °C) due to the combustion of CNTs except for CNT-CoNaX1, which shows a two-step weight loss with the inflection at approximate 480 °C. The rest can be considered as the catalyst after heat treatment. Generally, the decomposition of C_2H_2 on metal-supported catalysts leads to the formation of a mixture of CNTs and amorphous carbon on the catalyst surface, which can be identified as a two-step weight loss on TG curves. However, as shown in Fig. 3, with increasing Co content supported on the zeolite, CNT-CoNaX0, CNT-CoNaX2 and CNT-CoNaX3 exhibit an ensemble of non-amorphous carbon species tendency, indicating an excellent crystallinity of synthesized CNTs. This can be confirmed by former TEM result shown in Fig. 2.

The usual method to estimate the quantity of the deposited carbon during decomposition of small hydrocarbon molecules on metal-containing catalysts by CVD is calculated as follows:

$$\text{Carbon yield (\%)} = (m_{\text{tot}} - m_{\text{cat}})/m_{\text{cat}} \times 100 \%$$

where, m_{cat} is the initial amount of the catalyst (before reaction) and m_{tot} is the total weight of the sample after reaction. The estimation for the synthesized CNTs by different Co contents supported zeolite is given in Table-1.

Catalyst sample	Carbon yield %	Raman ratio (I_D/I_G)
CNT-CoNaX0	36.0	0.85
CNT-CoNaX1	35.4	0.76
CNT-CoNaX2	48.1	0.82
CNT-CoNaX3	60.4	0.78

Fig. 4 shows the Raman spectra of the synthesized CNTs observed under Nd-YAG laser of wavelength 1064 nm (excitation energy 2.41 eV) at 110 mW power.

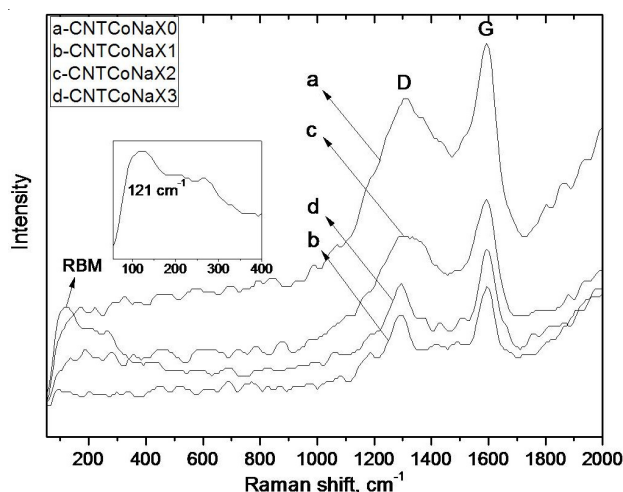


Fig. 4. Raman spectra of synthesized CNTs; (a) CNT-CoNaX0, (b) CNT-CoNaX1, (c) CNT-CoNaX2 and (d) CNT-CoNaX3

In all spectra for the synthesized CNTs, there are two characteristic peaks around the frequency of 1300 and 1590 cm^{-1} , which are identified as D- and G-bands, respectively. The G-band represents the tangential stretching (E_{2g}) mode of graphite and is related to the vibration of sp^2 -bonded carbon atoms in a two-dimensional hexagonal lattice; the D-band was associated with the disordered, sp^3 -hybridized carbon present as impurities and dispersive defects in the graphitic sheets²⁰. Here, it is obvious that G- and D-bands for all CNT samples both have a sharp single peak without other side peaks, indicating a good crystallinity of the wall layer of CNTs without more amorphous carbon or other impurities, in accordance with the result shown in Figs. 2 and 3. Moreover, this inference can be confirmed by the monolithic decrease tendency of the relative intensity ratios of the D- to G-bands (shown in Table-1) with increasing Co contents, because this ratio always is used as a measure of the degree of disorder in the graphite sheets and thus can be used for evaluating the crystallinity of the synthesized CNTs.

It is worth noting that at the frequency of approximate 121 cm^{-1} , there is a peak corresponding to the radial breathing mode (RBM), with the frequency dependent on the diameter of SWNTs, according to the relationship²¹ between the diameter (d) and the frequency (ω):

$$\omega_{\text{RBN}} = 224/d + 10 \text{ [nm]}$$

the Raman peak at 121 cm^{-1} corresponds to diameter of 2.0 nm.

Conclusion

High yield multi-walled carbon nanotubes (MWNTs) were synthesized on zeolite crystals (FAU) with Co catalysts by catalytic chemical vapour deposition (CCVD) using acetylene as the carbon source. During the ion-exchanging process, Na^+ cations in the faujasite-type zeolite NaX (FAU) have been completely exchanged by Co^{2+} cations. The inner and outer tube diameters of the typically synthesized MWNTs were in the range of 5.7-11.6 and 11.0-30.2 nm, respectively. With increasing Co content supported in the zeolite, the carbon yield showed a monotonic increasing tendency, reaching 60.4 % when the Co content was up to 11.5 wt%. And also we detected some SWNTs at around the frequency of 121 cm^{-1} (RBM) with Co content of 11.5 wt% whose diameter is *ca.* 2 nm.

ACKNOWLEDGEMENTS

This research was supported by National Research Foundation of Korea (NRF) through a grant (2010-0022504) provided by the Korean Government in 2010.

REFERENCES

- H.W. Zhu, C.L. Xu, D.H. Wu, B.Q. Wei, R. Vajtai and P.M. Ajayan, *Science*, **296**, 884 (2002).
- S. Iijima, *Nature*, **363**, 603 (1993).
- J. Kong, N.R. Franklin, C. Zhou, M.G. Chapline, S. Peng, K.J. Cho and H. Dai, *Science*, **287**, 622 (2000).
- A. Bachtold, P. Hadley, T. Nakanishi and C. Dekker, *Science*, **294**, 1317 (2001).
- P. Calvert, *Nature*, **399**, 210 (1999).
- A.C. Dillon, K.M. Jones, T.A. Bekkedahl, C.H. Kiang, D.S. Bethune and M.J. Heben, *Nature*, **386**, 377 (1997).
- W.I. Milne, K.B.K. Teo, G.A.J. Amaratunga, P. Legagneux, L. Gangloff, J.P. Schnell, V. Senmet, V.T. Binh and O. Groening, *J. Mater. Chem.*, **14**, 933 (2004).
- M. Corrias, B. Caussat, A. Ayrat, J. Durand, Y. Kihn, Ph. Kalck and Ph. Serp, *Chem. Eng. Sci.*, **58**, 4475 (2003).
- K.P. De Jong and J.W. Geus, *Catal. Rev.-Sci. Eng.*, **42**, 481 (2000).
- K. Hernadi, A. Fonseca, J.B. Nagy, D. Bernaerts, A. Fudala and A.A. Lucas, *Zeolites*, **17**, 416 (1996).
- W.Z. Li, S.S. Xie, L.X. Qian, B.H. Chang, B.S. Zou, W.Y. Zhou, R.A. Zhao and G. Wang, *Science*, **274**, 1701 (1996).
- K. Hernadi, A. Fonseca, J.B. Nagy, D. Bernaerts and A.A. Lucas, *Carbon*, **34**, 1249 (1996).
- Z. Konya, I. Vesselenyi, K. Lazar, J. Kiss and I. Kiricsi, *IEEE Trans. Nanotechnol.*, **3**, 73 (2004).
- I.J. Kim and H.J. Lee, *Key Eng. Mater.*, **280**, 891 (2005).
- H. Ago, S. Imamura, T. Okazaki, T. Saitoj, M. Yumura and M. Tsuji, *J. Phys. Chem. B*, **109**, 10035 (2005).
- M. Hulman, H. Kuzmany, O. Dubay, G. Kresse, L. Li, Z.K. Tang, P. Knoll and R. Kaindl, *Carbon*, **42**, 1071 (2004).
- S. Iijima, *Nature*, **354**, 56 (1991).
- A.R. Harutyunyan, *J. Nanosci. Nanotechnol.*, **9**, 2480 (2009).
- W. Zhao, D.N. Seo, H.T. Kim and I.J. Kim, *J. Ceramic Soc. (Japan)*, **118**, 983 (2010).
- L.D. Shao, G. Tobias, C.G. Salzmman, B. Ballesteros, S.Y. Hong, A. Crossley, B.G. Davis and M.L.H. Green, *Chem. Commun.*, 5090 (2007).
- A.M. Rao, J. Chen, E. Richter, U. Schlecht, P. C. Eklund, R.C. Haddon, U.D. Venkateswaran, Y.K. Kwon and D. Tomanek, *Phys. Rev. Lett.*, **86**, 3895 (2001).